COMPUTER ANIMATION AND VIRTUAL WORLDS
Comp. Anim. Virtual Worlds 2011; **22**:203–211
Published online 13 April 2011 in Wiley Online Library (wileyonlinelibrary.com). DOI: 10.1002/cav.392

SPECIAL ISSUE PAPER

3D body scanning with hairstyle using one time-of-flight camera

Jing Tong[1,2], Mingmin Zhang[1]*, Xueqin Xiang[1], Huaqing Shen[3], Hao Yan[1] and Zhengming Chen[2]

[1] State Key Laboratory of CAD&CG, Zhejiang University, China
[2] College of Computer & Information Engineering, HoHai University, China
[3] School of Arts, Zhejiang University, China

ABSTRACT

Capturing realistic 3D shapes of human bodies is very useful for many computer graphics applications. However, for existing 3D shape capturing devices, such as structured light, laser scanner or multi-view methods, problems arise when dealing with 3D hairstyle scanning and body deformation. To solve these problems, a novel approach is proposed to scan 3D body with hairstyle using only one time-of-flight (TOF) camera. By capturing depth data at video rate, temporal average meshes can be obtained from different views. After some analysis, we found that the local geometric details of real surfaces, after the hair scanning process and low-frequency body deformation, are still preserved in the average meshes. Utilising the restriction that the corresponding surfaces in different views should overlap, a global optimisation process is proposed to iteratively improve the average meshes, while still preserving the geometric details. The proposed system is compact, and can scan 3D human body easily. Copyright © 2011 John Wiley & Sons, Ltd.

KEYWORDS

time-of-flight camera; 3D body scanning; hairstyle; 3D shape reconstruction

***Correspondence**

Mingmin Zhang, State Key Laboratory of CAD&CG, Information Technology Building B, Zijingang Campus of Zhejiang University, Zhejiang University, China.
E-mail: zmm@cad.zju.edu.cn

1. INTRODUCTION

Many computer graphics applications, such as animation, computer games, human computer interaction and virtual reality, require realistic 3D models of human bodies. Using 3D scanning technology, such as structured light or laser scan, detailed human models could be created [1]. However, these devices are quite expensive and often require expert knowledge for their operation. Moreover, due to the reflected property and complicated geometry, hairstyle, though as an important characteristic of human beings, cannot be directly scanned using conventional 3D scanners. People are often asked to wear shower caps while scanning. This is not comfortable and the important hairstyle information is missing in the resulting 3D data. Another well-known problem is that it is difficult for people to stay rigid during the entire capturing process.

To capture realistic hairstyle information of a human being, image-based methods are almost the only options [2]. But this kind of methods are computationally expensive, and they have problems when there are sparse textures or complex occlusions among different views [3]. Even the state-of-the-art method [4] according to the Middlebury fails to properly reconstruct the 3D hairstyle in Figure 1a, where a girl rotating in front of a camera, with missing texture in the hair area and slight lighting changes among different views.

In fact, in many daily-applications, such as digital avatars, video game, online shopping, etc., an easy-to-use and robust 3D scanner to capture body shape with hairstyle is required. In addition, the user is allowed to undergo low-frequency non-rigid deformation. And the precision of outer hairstyle surface is just enough. To achieve this, in our method, TOF camera is utilised. At first glance of the captured data in Figure 1b, especially the noise and missing data around the hair area, one might argue that it is impossible to reconstruct body shape with hairstyle using one TOF camera. However, since the TOF camera is able to capture depth data at video rate, it is possible to use the information redundancy to refine the data.

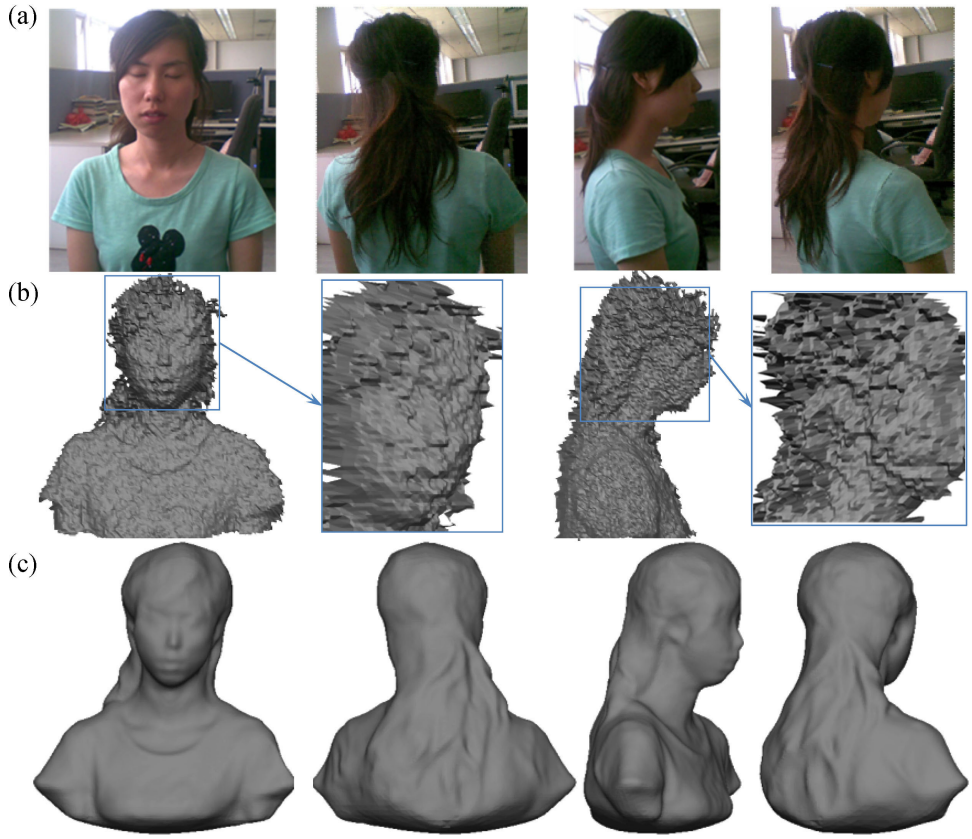

Figure 1. (a) Four out of eight colour pictures taken with similar view of the corresponding TOF camera, (b) the raw TOF data, (c) generated model using one TOF camera by the proposed method.

To the best of our knowledge, we present the first method to scan human body with hairstyle using one TOF camera. It is very easy to use, and can reconstruct body shape of reasonable quality in just a few minutes (Figure 1c). To achieve this, we present an optimisation method based on the refinement of temporal average meshes, which can solve 3D hair scanning and body deformation problems simultaneously. Finally, the hair fibres could be easily be generated according to several guide curves on the reconstructed hairstyle mesh (Figure 5), which can greatly reduce the artists' manual labour for styling hair fibres.

The main contributions are: (1) a 3D body scanning approach using one TOF camera. (2) The analysis that local geometric details of real surfaces are preserved in the average meshes. The experiments have shown the efficiency of our algorithm utilising this analysis. Our method can also scan static objects with normal material, and got very impressive results compared with the state-of-the-art method [5].

2. RELATED WORK

To get 3D models of human bodies, 3D scanning technology based on structured light and laser scan [6], or image-based methods [7] are both available. Generally, multiple meshes got from different views can be registered [8] and merged to form a complete 3D body mesh [9]. For low-frequency non-rigid errors caused by device non-linearities or calibration error, global non-rigid alignment approaches [10,11] are often applied. But owing to the reflected property and complicated geometry, the scanned hairstyle surface is too noisy, and seems not having a specific model to remove the noise. Therefore, hairstyle is thought not able to be directly scanned using conventional 3D scanners [2]. Furthermore, because of lack of texture in the hair area, image-based method [4] also fails in our experiment.

Researchers have also developed methods that may further capture hair fibres from multiple views and achieve highly realistic images [12,13]. But many of these methods require complex setup and will enlarge computing complexity. Reference [14] is the only literature we found that presents a scanning technique to reconstruct the geometry of a person's hairstyle. They can reconstruct geometry and reflectance of hair fibres. But their setup is in a light-stage fashion and the time and storage consuming is very large.

To solve these problems, TOF camera is used in our method. Compared with structured light, laser scan or stereo vision, TOF camera has great advantages. It enables

DOI: 10.1002/cav

acquiring depth data in real time with little considering about texture or lighting condition. The camera is compact, low-price and as easy-to-use as a video camera, which has the potential to be used by everyday users [15]. Unfortunately, the captured data cannot be directly used due to the low image resolution and high noise level.

Many works have been done to improve the data's quality. Reference [16] applied the traditional colour image super-resolution ideas to TOF cameras to obtain 3D data of higher X–Y resolution and less noise, which used depth images only. Reference [17] improved the accuracy of range maps with a probabilistic model based on the observation that the range map and intensity image measured by a TOF camera were linked by the shading constraint. Reference [3] proposed an integrated multi-view sensor fusion approach that combined information from multiple colour cameras and multiple TOF depth sensors. Reference [18] fused the complimentary characteristics of TOF camera and passive stereo, using dynamic MRFs with temporal coherence to improve the accuracy and robustness of depth estimates. Reference [19] generated a dynamic 3D human actor using a TOF camera. But they thought it was impossible to scan hairstyle surfaces, and the hair region was interpolated by the boundary curves. Currently, Reference [5] built the first 3D shape scanner based on a TOF camera. The algorithm is based on a combination of a 3D super resolution method with a probabilistic scan alignment approach that takes into account the sensor's noise characteristics. However, to the best of our best knowledge, none of existing methods could get 3D body shape with hairstyle of reasonable quality.

3. OUR ALGORITHM

The main pipeline of our algorithm is shown in Figure 2. In order to easily carry on the scanning of human body, a human will rotate in front of a TOF camera. For each view, the human is required to stay as still as possible for a few seconds, so that the camera can get multiple frames of data within a single view (Figure 2a). Among different views, the human is allowed to have low-frequency deformation. Temporal average meshes (Figure 2b) are generated for each view and rigid registered (Figure 2c). An iterative optimisation method is proposed to procedurally optimise the rigid matrices between different views and each view's output mesh (Figure 2d). Finally, reconstructed mesh (Figure 2e) is generated from the deformed average meshes.

4. DATA ACQUISITION

Figure 1b shows a frame of the raw data, which is very noisy, especially for the hair area. Figure 2a shows continuous captured multiple frames of a still body. In our experiment, after enough frames are captured, the accumulated data will visually contain the real surface.

Suppose t frames are captured for every r different view. Let m_i^j, $j = 1 \ldots t$, $i = 1 \ldots r$ denote the jth mesh captured in the ith view, $s_i = \frac{1}{t} \cdot \sum_{j=1}^{t} m_i^j$ denotes the average mesh of all frames in the ith view. When t is big enough, the coordinates of s_i tend to converge in our experiment. As illustrated in Figure 2b, s_i has captured some features of the hairstyle, and the data's quality has been greatly improved compared to Figure 1b.

5. ANALYSIS OF THE GEOMETRIC PROPERTY OF AVERAGE MESHES

Figure 3a and b show a close look at the average meshes of two different views, s_i and s_k. Individually, they all capture some good characteristic of the hairstyle, and resemble to the corresponding pictures in Figure 4a. But when looking at the corresponding areas of s_i and s_k, for example, depicted in the yellow squares, the corresponding shapes look very different. The one in s_i is more flat, while the one in s_k is more concave. The reason causing this phenomenon is analysed in Figure 3c.

Let ξ be the exact outer surface to be measured, ξ' is the other boundary of the region that has effects on the

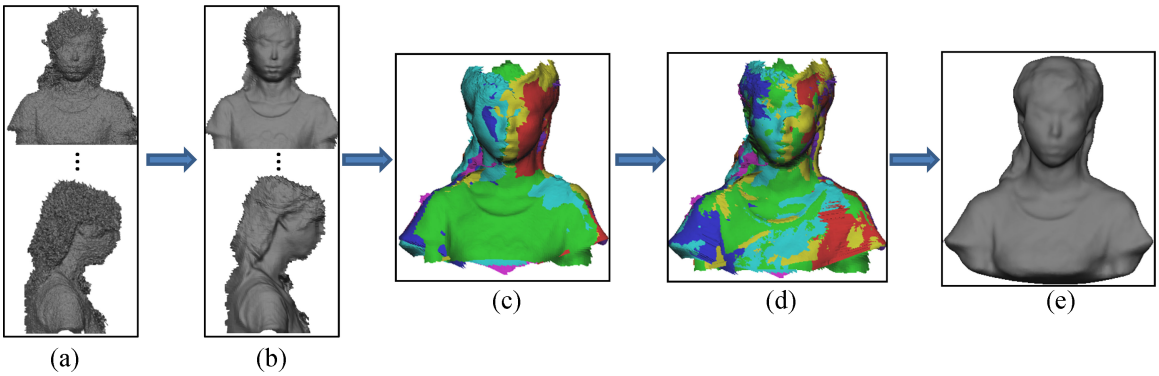

Figure 2. The main pipeline of our algorithm. (a) Multiple frames of raw TOF data for separated views, (b) the average meshes for different views, (c) average meshes after initial rigid registration, (d) average meshes after further optimisation, (e) reconstructed mesh.

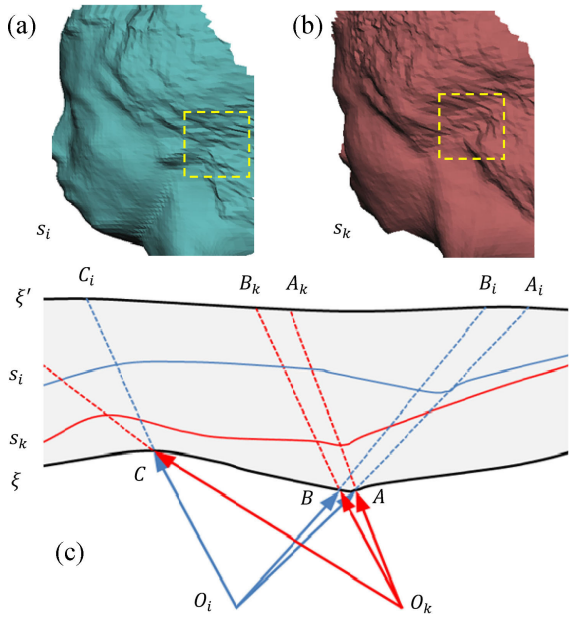

Figure 3. Close look of the average meshes in two different views s_i(a) and s_k(b); (c) the analysis of geometric property of the average meshes.

measured data. (For the skin area, simply let $\xi' = \xi$). Multiple frames are captured from separated viewpoints O_i, O_k, and then average meshes s_i, s_k are got. Let $d_i = s_i - \xi$ denotes the difference between s_i and ξ, and d_i lies mainly in the viewing direction. For the sample point A, A_i is the intersection of extension of O_iA and ξ'. The measurement error $d_i|_A$ will be mainly determined by the local property of the neighbourhood of AA_i, which can be written as $d_i|_A \sim \text{LocalProperty}(AA_i)$. For the sample point B close to A, there also exists $d_i|_B \sim \text{LocalProperty}(BB_i)$. Since AA_i and BB_i are geometrically close, their local property has great possibility to be similar, so are the values of $d_i|_A$ and $d_i|_B$. Therefore, in the neighbourhood of a sample point A, the local geometry of average mesh s_i has great possibility to be similar to the real surface ξ. This is why an average mesh is visually decent.

But for a sample point C far from A, CC_i are geometrically away from AA_i. Their local properties are likely to be different, so are $d_i|_C$ and $d_i|_A$. s_i will differ from ξ in a macroscopic view. Likewise, to measure A from viewpoint O_k, we have $d_k|_A \sim \text{LocalProperty}(AA_k)$. When ξ' is not close to ξ, for example, in the hair area, AA_k are geometrically away from AA_i, $d_k|_A$ has great possibility to be different from $d_i|_A$. Thus the corresponding areas in Figure 3a, b may look very different.

In practice, it is impossible for human body to stay rigid during the entire capturing process. Thus, in our assumption, the human body is allowed to undergo low-frequency non-rigid deformation among different views. In this situation, just like the hair scanning problem discussed above, the high-frequency geometric details are also well preserved after the deformation.

To refine the coordinates of average meshes, the restriction that the corresponding areas in s_i, s_k should overlap can be utilised, and local geometric details of s_i, s_k should also be preserved during the optimisation process.

6. ENERGY FUNCTION TO REFINE AVERAGE MESHES

Let $S = \{s_i | i = 1 \dots r\}$ be the average meshes, $Xf = \{xf_i | i = 1 \dots r\}$ be the rigid matrices used to register r different views. For simplicity, let S denote the average meshes applied by Xf. To further improve the coordinates of average meshes S and rigid matrices Xf, we resort to the following energy function to be minimised:

$$E(S) = E_{\text{localfeature}}(S) + \alpha \cdot E_{\text{dist}}(S) + \beta \cdot E_{\text{spring}}(S) \quad (1)$$

where $E_{\text{localfeature}}(S) = \sum_{i=1}^{r} E_{\text{localfeature}}(s_i)$ preserves the local geometric details of S; $E_{\text{dist}}(S) = \sum_{corr(s_i,s_k)} E_{\text{dist}}(s_i, s_k)$ makes the corresponding areas of different average meshes overlap; $E_{\text{spring}}(S) = \sum_{i=1}^{r} E_{\text{spring}}(s_i)$ is a regularising term that helps guide the optimisation to a desirable local minimum; α, β are weighted coefficients.

Average mesh s_i is described as (K_i, V_i), where K_i reprent the connectivities and $V_i = \{v_i^1, \dots, v_i^n\}$ are the vertices. N_l describes the 1-ring neighbourhood of vertex v_i^l, and d_l is its degree. As the depth image is regular sampled, similar to the definition in Reference [20], the Laplacian coordinate for v_i^l is defined as:

$$\delta_l = v_i^l - \frac{1}{d_l} \sum_{m \in N_l} v_i^m \quad (2)$$

Let A be the adjacency matrix, $D = \text{diag}(d_1, \dots, d_n)$, $L = I - D^{-1}A$, $v_i^{l'}$ be the new vertex after optimisation. Then we have

$$E_{\text{localfeature}}(s_i) = \sum_{l=1}^{n} \left\| T_l \delta_l - L(v_i^{l'}) \right\|^2 \quad (3)$$

T_l is a local transformation matrix, and is calculated by minimising

$$\sum_{m \in \{l\} \cup N_l} \left\| T_l v_i^m - v_i^{m'} \right\|^2 \quad (4)$$

For two average meshes have corresponding areas, we have $E_{\text{dist}}(s_i, s_k) = \sum_{cor(v_i^l, v_k^m)} \left\| v_i^l - v_k^m \right\|^2$, where $cor(v_i^l, v_k^m)$ denotes that v_i^l and v_k^m are corresponding vertices of s_i and s_k, and can be found similar to the iterative closest points (ICP) method [8]. Let u_i^l denote the middle point of (v_i^l, v_k^m), then for s_i, we have the following energy to be minimised:

$$E_{\text{dist}}(s_i) = \sum_{cor(v_i^l, u_i^l)} \left\| v_i^l - u_i^l \right\|^2 \quad (5)$$

$E_{\text{spring}}(s_i)$ is the sum square of all edges' length, and is utilised to guide the optimisation to a desirable local minimum.

$$E_{\text{spring}}(s_i) = \sum_{\{l,m\} \in K_i} \left\| v_i^l - v_i^m \right\|^2 \quad (6)$$

DOI: 10.1002/cav

Figure 4. Reconstructed models in different views with the corresponding pictures.

7. MINIMISING THE ENERGY FUNCTION

Because only one TOF camera is used in our method, the rigid matrices of different views are unknown. In an average mesh, the noise level of the hair area is far more significant than the other area. Thus, for two average meshes s_i, s_k, surfaces except the hair area are used to get the initial rigid matrices xf_i, xf_k. The new vertices are then generated by solving a sparse linear system formed by Equations (1)–(6). An iterative method is finally utilised to minimise the energy function as follows:

Optimise(s_i, s_k, xf_i, xf_k) {
Fix xf_i, xf_k, optimise s_i, s_k by solving a sparse linear system formed by Equations (1)–(6).
Fix s_i, s_k, use ICP method to refine xf_i, xf_k.
} until convergence

To optimise $S = \{s_i | i = 1 \ldots r\}$, $Xf = \{xf_i | i = 1 \ldots r\}$ got from multiple views, a global multi-view registration method is used to get the initial rigid matrices [21], and average meshes are optimised with each other pair wisely. To solve the error accumulation problem, a global matrix system lists all the average meshes' constraints as diagonal sub-matrices can be formed similar to Reference [22]. The energy function $E(S)$ is minimised by optimising all average meshes simultaneously:

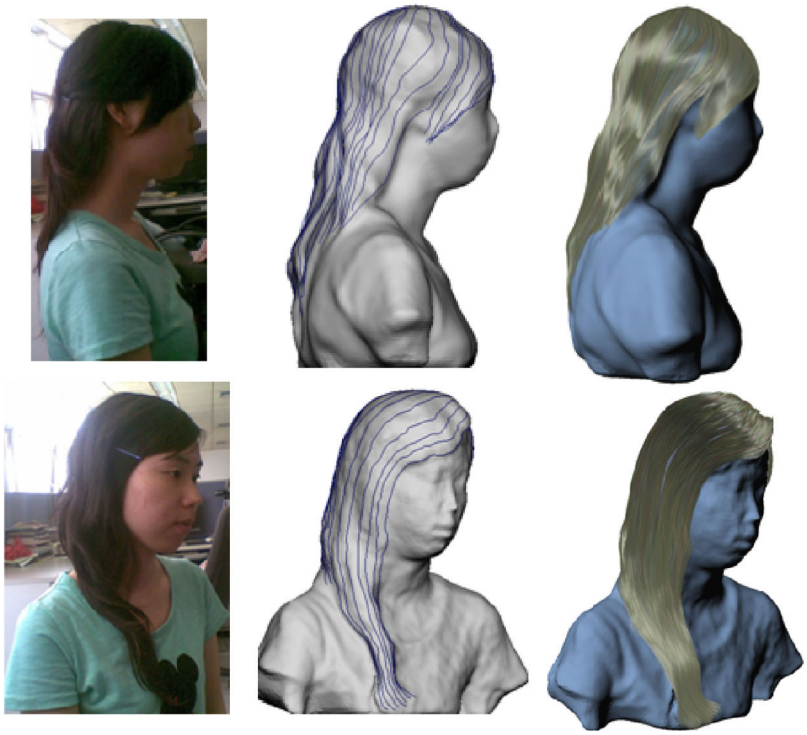

Figure 5. The corresponding pictures, reconstructed models with guide curves and interpolated hair fibres.

Optimise(*S*,*Xf*) {
Fix *Xf*, optimise *S* by solving a global linear system.
Fix *S*, use global ICP method to refine *Xf*.
} until convergence

The original and optimised average meshes are shown in Figure 2c, d (each with different colours). We can conclude that after the optimisation, the corresponding areas in different average meshes tend to overlap. Finally, Poisson Surface Reconstruction [10] is employed to get a complete 3D model.

8. RESULTS

A person will rotate for about 360° in front of a TOF camera in our experiment. For eight views, separated by about 45°, the person is asked to be as still as possible for about 2 seconds, so that the camera may get 100 frames for each view. Though slight movement is inevitable within a single view, the resulting average mesh is feasible in our experiment. Due to the low resolution of raw depth image, only upper body is captured in our experiment. To fully capture the whole body, the upper and lower parts can be scanned separately, and the similar process will carry on.

Our system uses a MESA Swissranger SR4000 sensor [23], which can capture depth and intensity images up to 54 frames per second, with the resolution of 176×144 pixels. For a single frame, the depth image is naturally with a grid structure, which can be easily transformed to a triangle mesh. First, a depth and amplitude threshold method is used to roughly segment the foreground data and remove points which are either too dark or too bright. Then, sliver faces followed by vertices not referenced by any face are deleted.

Figure 4 shows the results of testing our algorithm by data of long straight hair, long curve hair, short hair and ponytails. To guide the optimisation to a desirable local minimum, we set $\alpha = 0.01$, $\beta = 1$ at the first iteration. As the optimisation converges to the solution, the influence of $E_{\text{localfeature}}$ and E_{spring} can be gradually reduced. We finally set $\alpha = 1$, $\beta = 0$. In our experiment, the iteration stops after 4–7 steps when the energy function stops decreasing obviously. Our platform is Intel Core 2 Q9550, 4G RAM, NVIDIA GTX280. The computing time is statistic in Table 1. Since it is hard to get the ground truth of hairstyle surface, we simply let error ε be the average distance of all corresponding vertices on different average meshes. After the optimisation, ε has been obviously decreased.

To further generate hair fibres, Reference [24] uses the outer hairstyle and scalp meshes as boundaries, and hair fibres are generated in the hair volume based on a shape matching algorithm. While in 3D animation production,

Table 1. Average distance and computing time.

Figures	1	6a	6b	6c	6d	6e
ε (cm) before optimisation	1.4	1.7	2.3	1.8	1.1	4.5
ε (cm) after optimisation	0.3	0.4	0.8	0.6	0.4	1.0
Computing time (min)	1.8	1.2	2.7	1.5	1.0	3.2

DOI: 10.1002/cav

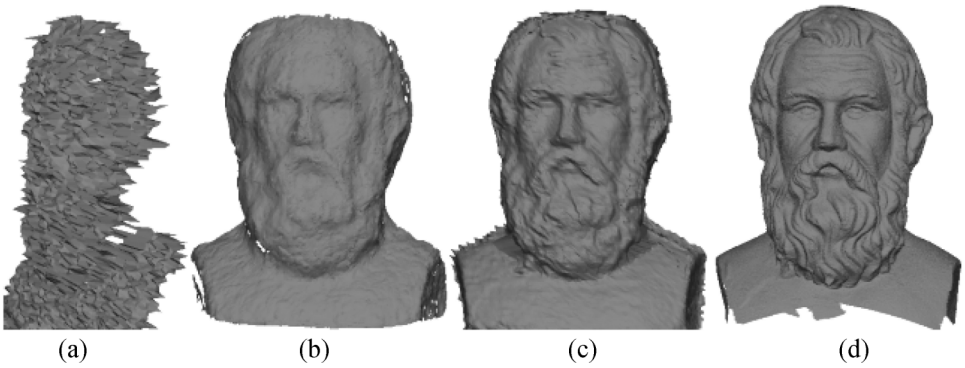

Figure 6. (a) Raw TOF data, (b) model obtained by Reference [5], (c) model obtained by our method, (d) laser scan.

hair fibres are often generated (interpolated) and edited by some 3D guide curves. It is difficult to draw 3D guide curves to get realistic hairstyle with only 2D pictures as reference. By using our method, guide curves can be easily drawn on the reconstructed hairstyle mesh, which will greatly reduce the artists' manual labour for styling realistic hair fibres. As shown in Figure 5, even a beginner can easily draw the guide curves on the reconstructed mesh and get hair fibres of reasonable quality in several minutes.

Furthermore, our method can also deal with static objects with normal material. We have tested our algorithm with still sculpture data provided by Reference [5]. The average distance of corresponding vertices from Figure 6b to 6d is 0.4, while the average distance from Figure 6c to 6d is 0.3. Compared with the laser scan data, our method can get models with similar geometric details of reasonable quality. Moreover, the computing time is about 2 minutes, while Reference [5] is around 330 minutes with a MATLAB implementation.

The reason that our algorithm can get such results is analysed below. The data captured by TOF camera contain high-level random noise and non-trivial systematic bias. Through temporal averaging, random noise is effectively reduced. The systematic bias is pixel dependent and could be modelled as an offset d_i in the viewing direction. d_i is dependent on many factors, including the scene reflectance, surface orientation, distance, etc. [25]. Reference [5] makes a simplifying assumption that d_i increases with the radial distance and ignores other factors. For our method, as long as the relevant properties are continuous for the scanned object, the analysis of average meshes also works considering the corresponding factors. Therefore, for the sculpture in Figure 6, systematic bias caused by more factors can be corrected using our method.

9. CONCLUSION

Though as an important characteristic of a human being, 3D hairstyle scanning is thought to be impossible by most researchers. In this paper, a new approach is presented to easily scan 3D body with hairstyle using one TOF camera. An optimisation method is developed to solve the hair scanning and body deformation problems simultaneously. The method has greatly broadened the scope of usage of TOF camera, and can be applied for HCI, digital avatars, video game, animation and many other applications. However, the quality of the reconstructed model is still low for some applications. Problems also arise where the hair is too thin, for instance, the tips of ponytails. In the future, we plan to investigate approaches by combining TOF camera with image-based methods, as well as reconstructing 3D shape of dynamic hairstyle.

ACKNOWLEDGEMENTS

This work was co-supported by the 863 Programme of China (No. 2009AA062700), the NSFC Project (No. 60775027) and Doctoral Science Foundation of Hohai University (No. XZX/09B005-05) Key HighTech project of Zhejiang Province (2009C11SA640034). The authors would like to thank Jiejie Zhu, Ruigang Yang and Ligang Liu for the helpful discussion. The authors would also thank Juying Cai, Lizhen Han and Hongbo Tian for being models in the experiments.

REFERENCES

1. Allen B, Curless B, Popovic Z. The space of human body shapes: reconstruction and parameterization from range scans. *ACM Transactions on Graphics* 2003; **22**(3): 587–594.
2. Kelly W, Florence B, Tae-Yong K, Stephen RM, Marie-Paule C, Ming CL. A survey on hair modeling: Styling, simulation, and rendering. *IEEE Transactions on Visualization and Computer Graphics* 2007; **13**: 213–234.
3. Kim YM, Theobalt C, Diebel J, Kosecka J, Miscusik B, Thrun S. Multi-view image and tof sensor fusion for dense 3d reconstruction. In *IEEE 12th International Conference on Computer Vision Workshops (ICCV Workshops)*, 2009; pages 1542–1549.
4. Furukawa Y, Ponce J. Accurate, dense, and robust multi-view stereopsis. *Proceedings of the IEEE Computer Society Conference on Computer Vision and Pattern Recognition*, 2007; pages 2118–2125.

5. Cui Y, Schuon S, Chan D, Thrun S, Theobalt C. 3D shape scanning with a time-of-flight camera. *Proceedings of the IEEE Computer Society Conference on Computer Vision and Pattern Recognition*, 2010; pages 1173–1180.
6. Douglas L, Gabriel T. Build your own 3D scanner: 3D photography for beginners. *ACM SIGGRAPH 2009 Courses, SIGGRAPH '09*, 2009; pages 1–94.
7. Seitz SM, Curless B, Diebel J, Scharstein D, Szeliski R. A comparison and evaluation of multi-view stereo reconstruction algorithms. *Proceedings of the IEEE Computer Society Conference on Computer Vision and Pattern Recognition*, 2006; pages 519–528.
8. Rusinkiewicz S, Levoy M. Efficient variants of the icp algorithm. In *Third International Conference on 3D Digital Imaging and Modeling (3DIM)*, 2001; pages 145–152.
9. Bolitho M, Kazhdan M, Burns R, Hoppe H. Parallel poisson surface reconstruction. In *Advances in Visual Computing*, *Lecture Notes in Computer Science*, Vol. 5875. Springer-Verlag: Berlin, Heidelberg, 2009; 678–689.
10. Brown BJ, Rusinkiewicz S. Global non-rigid alignment of 3-d scans. *ACM Transactions on Graphics* 2007; **26**: 21:1–21:9.
11. Myronenko A, Song X. Point-set registration: coherent point drift. *IEEE Transactions on Pattern Analysis and Machine Intelligence* 2009; **32**: 2262–2275.
12. Wei Y, Ofek E, Quan L, Shum H-Y. Modeling hair from multiple views. *ACM Transactions on Graphics* 2005; **24**: 816–820.
13. Jakob W, Moon JT, Marschner S. Capturing hair assemblies fiber by fiber. *ACM Transactions on Graphics* 2009; **28**: 164:1–164:9.
14. Paris S, Chang W, Kozhushnyan OI, *et al*. Hair photobooth: geometric and photometric acquisition of real hairstyles. *ACM Transactions on Graphics* 2008; **27**: 30:1–30:9.
15. Kolb A, Barth E, Koch R, Larsen R. Time-of-flight sensors in computer graphics. *Computer Graphics Forum* 2010; **29**(1): 141–159.
16. Schuon S, Theobalt C, Davis J, Thrun S. High-quality scanning using time-of-flight depth superresolution. In *2008 IEEE Computer Society Conference on Computer Vision and Pattern Recognition Workshops*, Vols 1–3.
17. Bohme M, Haker M, Martinetz T, Barth E. Shading constraint improves accuracy of time-of-flight measurements. *Computer Vision And Image Understanding* 2010; **114**(12): 1329–1335.
18. Zhu J, Wang L, Gao J, Yang R. Spatial-temporal fusion for high accuracy depth maps using dynamic mrfs. *IEEE Transactions on Pattern Analysis and Machine Intelligence* 2010; **32**(5): 899–909.
19. Cho J-H, Kim S-Y, Ho Y-S, Lee K. Dynamic 3d human actor generation method using a time-of-flight depth camera. *IEEE Transactions on Consumer Electronics* 2008; **54**(4): 1514–1521.
20. Sorkine O, Cohen-Or D, Lipman Y, Alexa M, Rossl C, Seidel H-P. Laplacian surface editing. *Proceedings of the 2004 Eurographics/ACM SIGGRAPH Symposium on Geometry Processing* 2004; **71**: 175–184.
21. Pulli K. Multiview registration for large data sets. In *Second International Conference on 3D Digital Imaging and Modeling*, 1999; pages 160–168.
22. Miao L, Qing Z, Huamin W, Ruigang Y, Minglun G. Modeling deformable objects from a single depth camera. In *IEEE 12th International Conference on Computer Vision*, 2009; pages 167–174.
23. SR4000 user manual, 2010. MESA Imaging AG.
24. Sobottka G, Kusak M, Weber A. Hairstyle construction from raw surface data. *Proceedings of the International Conference on Computer Graphics, Imaging and Visualisation*, 2006; pages 365–371.
25. Kim YM, Chan D, Theobalt C, Thrun S. Design and calibration of a multi-view tof sensor fusion system. In *2008 IEEE Computer Society Conference on Computer Vision and Pattern Recognition Workshops*, Vols 1–3.

AUTHORS' BIOGRAPHIES

Jing Tong received the Bachelor's degree in Applied Mathematics at Shandong University in 2003 and the Master's degree in Operational Research and Control Theory at Shandong University in 2006. From 2006, he has been teaching and researching at Hohai University. Now he is an assistant professor of the Computer and Information Engineering College. He is also a PHD student of Zhejiang University. His personal research domain and interests are Computer graphics and Computer Vision.

Mingmin Zhang is an associate professor of Computer and Engineering Department, Zhejiang University. She got the Bachelor degree from Computer Science Dept, Nanjing University in 1990, and the Master and PhD degree from Computer Science and Engineering Department, Zhejiang University in 1995 and 2008. She has published more than 30 papers on international journals, national journals, and conferences in recent years. She is the co-author of two books related to computer graphics and multimedia. Her research interests include: Virtual reality/Virtual environment, multi-resolution modeling, real-time rendering, distributed VR, Visualization, Multimedia and Image processing.

DOI: 10.1002/cav

Xueqin Xiang received the Bachelor's degree in computer science at Hangzhou Dianzi University in 2003 and the Master's degree in pattern recognition and artificial intelligence at Hangzhou Dianzi University in 2008. From 2008, he has been working for his PHD's degree at the state key lab of computer-aided design and computer graphics, Zhejiang University. His personal research domain and interests are computer vision, depth camera and etc. He has published over 10 technical papers.

Huaqing Shen received the Bachelor's degree in physics science at Hangzhou University in 1990 and the Master's degree in chemistry at Chinese Academy of Sciences in 1993. Now he is an associate professor of Computer and Engineering Department, Zhejiang University. His research interests include are Virtual reality, Visualization and animation.

Hao Yan received the Bachelor's degree in educational technology at Suzhou University in 2010. Now he is a master student of computer science and technology in Zhejiang University. His research domain and interests are computer vision, human–computer interaction and etc.

Zhengming Chen is a professor and the director head of Department of Computer Science in College of Computer & Information Engineering, Hohai university (ChangZhou). He received his PhD degree from Zhejiang University, China, in 2001. Currently his research interests are focus on feature modeling and recognition, CAD/CAM integration, Computer Graphics and Virtual Reality. He has successfully conducted National High Technology Research and Development 863 Program of China, and National Natural Science Foundation of China. He has authored or co-authored more than 60 papers in the top scientific journals, and conference proceedings.